

---

# Minimum Spanning Tree cluster analysis of the LMC region above 10 GeV: detection of the SNRs N 49B and N 63A

R. Campana • E. Massaro • E. Bernieri

**Abstract** We present the results of a cluster search in the  $\gamma$ -ray sky images of the Large Magellanic Cloud region by means of the Minimum Spanning Tree algorithm at energies higher than 10 GeV, using 9 years of *Fermi*-LAT data. Several significant clusters were found, the majority of which associated with previously known  $\gamma$ -ray sources. New significant clusters associated with the supernova remnants N 49B and N 63A are also found, and confirmed with a Maximum Likelihood analysis of the *Fermi*-LAT data.

**Keywords**  $\gamma$ -rays: observations –  $\gamma$ -rays: source detection

## 1 Introduction

The Large Magellanic Cloud (LMC) is a very interesting target for  $\gamma$ -ray astronomy since the early suggestion by Ginzburg (1972), subsequently developed by Ginzburg and Ptuskin (1984), who proposed to observe the Magellanic Clouds at high energies to test the hypothesis on the metagalactic origin of cosmic rays via the  $\pi^0$  decay process. The  $\gamma$ -ray emission from LMC was discovered by EGRET-CGRO (Sreekumar et al. 1992).

The large amount of data collected by the *Fermi*-Large Area Telescope (LAT) instrument (Ackermann

et al. 2012) in almost ten years of operation allows not only this type of studies but also the possibility to search for localized emission regions and point-like sources, that are particularly bright at energies in the GeV band and higher. The H.E.S.S. collaboration reported (H.E.S.S. Collaboration et al. 2015) observations of three sources up to about 10 TeV in the LMC, two of them associated with the Supernova Remnants (SNR) N 157B (H.E.S.S. Collaboration et al. 2012) and N 132D, the former containing the highest known spin-down luminosity pulsar PSR J0537–6910 (Marshall et al. 1998; Cusumano et al. 1998) with the fast period of 16 ms.

An analysis of the *Fermi*-LAT data of the first 6 years from the LMC was presented by Ackermann et al. (2016) who detected four point sources (P1 to P4): one corresponding to the pulsar PSR J0540–6919 (*Fermi* LAT Collaboration et al. 2015), and two associated with the SNRs N 157B and N 132D, while one source (P3) has been recently identified with the first extragalactic  $\gamma$ -ray binary within the SNR DEM L241 (Corbet et al. 2016).

In a series of papers (Bernieri et al. 2013; Campana et al. 2015, 2016c,b,a, 2017) we applied successfully the Minimum Spanning Tree (hereafter MST, Campana et al. 2008, 2013) source-detection method for searching new  $\gamma$ -ray sources closely associated with known BL Lac objects and blazar candidates, and illustrated how MST works in finding clusters having a small number of photons, but likely related to point-like sources.

In this paper we present the results of a MST analysis aimed at detecting photon clusters in the *Fermi*-LAT data acquired in 9 years of observation above 10 GeV in a sky region containing the LMC, in order to identify candidate sources in the high energy  $\gamma$ -rays. It should be emphasized that the dataset analyzed in this paper has a significant longer exposure than the previous *Fermi*-LAT studies (Ackermann et al. 2016), and

---

R. Campana

INAF/OAS-Bologna, via Gobetti 93, I-40129, Bologna, Italy.

E. Massaro

INAF/IAPS-Roma, via del Fosso del Cavaliere 100, I-00133, Roma, Italy

In Unam Sapientiam, Roma, Italy

E. Bernieri

INFN/Sezione di Roma Tre, Roma, Italy

Department of Mathematics and Physics, University of Roma Tre, Roma, Italy.

employs the much improved Pass 8 event processing (Atwood et al. 2013).

In particular, we found some evidence for possible extended structures and studied which cluster parameters can be used to discriminate them from patterns originated by pointlike sources. Moreover, our results indicate the occurrence of significant photon clustering close to the position of some bright SNRs not previously associated with  $\gamma$ -ray emitters.

The outline of this paper is as follows. In Section 2 the MST algorithm is briefly described, while the analysis of the LMC region is presented in Section 3. In Section 4 we deepen the analysis of some interesting SNR counterparts to MST clusters, while in Section 5 the results are summarized.

## 2 Photon cluster detection by means of the MST algorithm

The MST is a topometric algorithm employed for searching clusters in a field of points. A brief description of the method was presented in Campana et al. (2015), while a more detailed description with the statistical properties can be found in Campana et al. (2008, 2013). In this section the principal characteristics of the MST method are summarized for the sake of completeness.

Considering a two-dimensional set of  $N_n$  points, or *nodes*, the set  $\{\lambda_i\}$  of weighted edges connecting them can be defined. The MST is the unique *tree* (a graph without closed loops) connecting all the nodes with the minimum total weight,  $\min[\sum_i \lambda_i]$ . The edge weights, in the case of a region on the celestial sphere, are the angular distances between photon arrival directions.

Once the MST is computed, a set of subtrees corresponding to clusters of photons is extracted by means of the two following operations (*primary* selection): *i) separation*: removing all the edges having a length  $\lambda \geq \Lambda_{\text{cut}}$ , the separation value, that can be defined in units of the mean edge length  $\Lambda_m = (\sum_i \lambda_i)/N_n$  in the MST, to obtain a set of disconnected sub-trees<sup>1</sup>; *ii) elimination*: removing all the sub-trees having a number of nodes  $N \leq N_{\text{cut}}$ , leaving only the clusters having a size over a properly fixed threshold. The remaining set of sub-trees provides a first list of candidate clusters. A *secondary* selection must be applied for extracting the most robust candidates for  $\gamma$ -ray sources. In Campana et al. (2013) a suitable parameter for this selection was introduced, the so-called cluster *magnitude*:

$$M_k = N_k g_k \quad (1)$$

where  $N_k$  is the number of nodes in the cluster  $k$  and the *clustering parameter*  $g_k$  is the ratio between  $\Lambda_m$  and  $\lambda_{m,k}$ , the mean length over the  $k$ -th cluster edges. The probability to obtain a given magnitude value combines that of selecting a cluster with  $N_k$  nodes together with its “clumpiness” with respect to the mean separation in the field. On the basis of comparative tests performed in simulated and real *Fermi*-LAT fields, Campana et al. (2013) found that  $\sqrt{M}$  has a linear correlation with other statistical source significance parameters, e.g. those derived from a wavelet-based algorithm or Maximum Likelihood (Mattox et al. 1996) analysis, and therefore it can be a good estimator of statistical significance of MST clusters. In particular, a lower threshold value of  $M$  around 15–20 would reject the large majority of spurious low-significance clusters.

Other characteristic parameters for the clusters can be then computed. Examples are the centroid coordinates, obtained by means of a weighted mean of the cluster photon arrival directions (see Campana et al. 2013) and the radius of the circle centred at the centroid and containing the 50% of photons in the cluster, the *median radius*  $R_m$ . The latter parameter, for a cluster that can be associated with a genuine pointlike  $\gamma$ -ray source, should be smaller than or comparable to the 68% containment radius of instrumental Point Spread Function (PSF). This radius varies from 0 $^{\circ}$ .2 at 3 GeV to 0 $^{\circ}$ .14 at 10 GeV in the case of a bright source for diffuse class front-observed events (Ackermann et al. 2013). Moreover, it can also be expected that the angular distance between the positions of the cluster centroid and the possible optical counterpart are lower than the latter value. Another useful parameter for understanding the structure of a cluster is its *maximum radius*  $R_{\text{max}}$ , defined as the distance between the centroid and the farthest photon in the cluster, which is expected to be of some arcminutes for a point-like source and a few tens of arcminutes either for extended structures or for unresolved close pairs of sources.

## 3 Cluster analysis of LMC high energy $\gamma$ -ray data

LAT data (Pass 8R2) above 10 GeV, covering the whole sky in the 9.0 years time range from the start of mission (2008 August 04) up to 2017 August 04, were downloaded from the FSSC archive<sup>2</sup>. Standard cuts on the zenith angle, data quality and good time intervals were applied. Then, a region 12 $^{\circ}$   $\times$  9 $^{\circ}$  approximately centered at the LMC was selected and the MST algorithm was

<sup>1</sup>Throughout this paper the simplifying convention to write for instance  $\Lambda_{\text{cut}} = 0.7$  instead of  $\Lambda_{\text{cut}} = 0.7\Lambda_m$  will be used.

<sup>2</sup><http://fermi.gsfc.nasa.gov/ssc/data/access/>

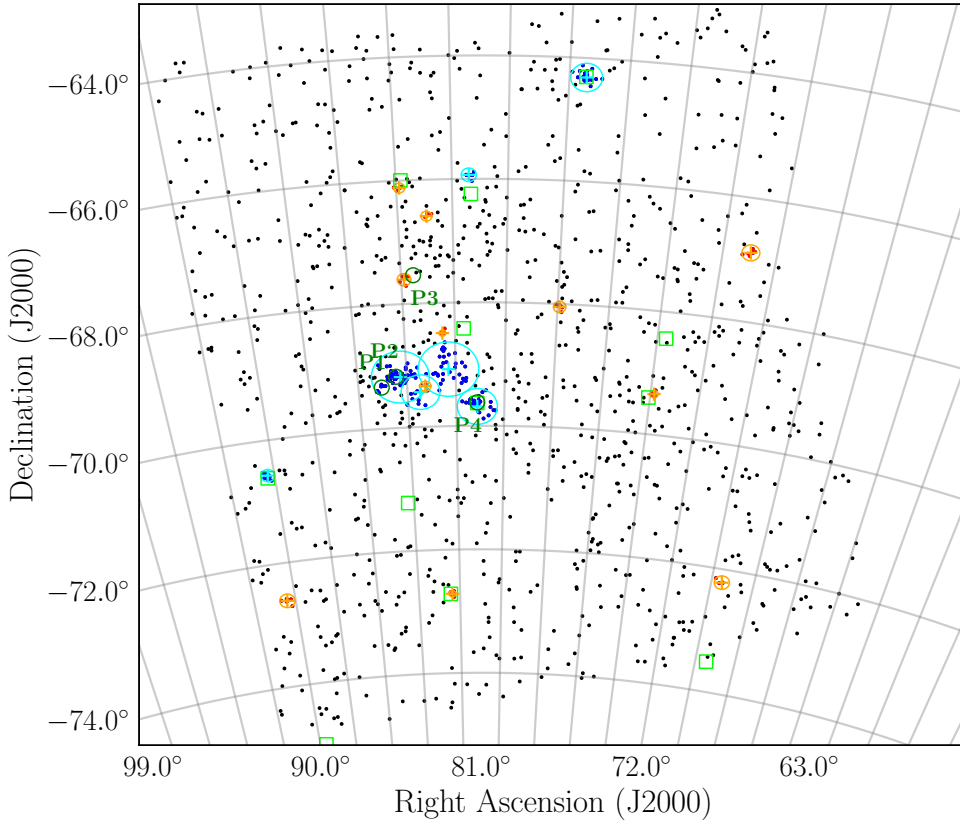


**Fig. 1** Photon map in equatorial coordinates of the sky region ( $12^\circ \times 9^\circ$  in a Galactic coordinate frame) centered at LMC at energies higher than 10 GeV. Blue and red points are the photons corresponding to the high and low significance clusters in Tables 1 and 2. Symbol codes are: position of the MST high significance clusters above 10 GeV (cyan crosses), MST low significance clusters (orange crosses), 3FGL sources (light green open squares),  $\gamma$ -ray point sources P1–P4 found by Ackermann et al. (2016) (open green circles). The cyan and orange circles are centered on the MST centroids and have a radius equal to  $R_{\max}$ .

applied. Figure 1 shows the photon map in this region at energies higher than 10 GeV.

MST was first applied to the  $>10$  GeV sky with  $\Lambda_{\text{cut}} = 0.7$ , and  $N_{\text{cut}} = 3$ , while the secondary selection was used to select significant concentrations only. The choice of the optimal  $\Lambda_{\text{cut}}$  is not a simple task, because of the presence of a diffuse and non-homogeneous emission in the LMC (Ackermann et al. 2016) which can make difficult to resolve nearby clusters. We thus performed other analyses with shorter  $\Lambda_{\text{cut}}$  values to compare the results with those of the longer separation length.

The secondary selection was performed by adopting different thresholds for different cluster sizes (see Table 1 for a summary). For clusters having a number of photons  $N > 5$ , a threshold of  $M \geq 20$  was adopted, while for clusters having  $N = 4$  and  $N = 5$  nodes, a threshold of  $g \geq 3.5$  and  $g \geq 3.0$  (corresponding to  $M \geq 14$  and  $M \geq 15$ , respectively) was chosen in order to extract only structures with a photon density

much higher than the surrounding and reduce in this way the probability for random clustering, as suggested by numerical simulations (Campana et al. 2013). We also extended our analysis to low significance clusters ( $M < 20$ ), because of the possible associations either with extended features, or with faint sources, as verified by *a posteriori* comparisons with literature data sets. According to Campana et al. (2013) we expect that a percentage of around 50% of these low significance and “poor” clusters could be spurious and therefore those expected to be associated with an interesting counterparts must be validated by further analysis.

**Table 1** Criteria for the secondary selection

Cluster size	Selection criterium
$N > 5$	$M \geq 20$
$N = 5$	$g \geq 3.5$
$N = 4$	$g \geq 3.0$

**Table 2** Coordinates and main properties of MST clusters with  $M > 20$  detected in the LMC sky region at energies higher than 10 GeV. Celestial coordinates are J2000, angular distances  $\Delta\theta$  are computed between the centroids of MST clusters and those of indicated counterparts. The first section reports clusters detected using  $\Lambda_{\text{cut}} = 0.7$ , while the lower section those found with  $\Lambda_{\text{cut}} = 0.5$ . The letter “e” indicates likely extended structures, see main text for details.

RA °	Dec °	$l$ °	$b$ °	$N$	$g$	$M$	$R_m$ ′	$R_{\text{max}}$ ′	$\Delta\theta$ ′	Possible counterparts
$\Lambda_{\text{cut}} = 0.7$										
77.427	−64.315	274.307	−35.210	20	3.129	62.576	4.4	13.6	2.4	FL8Y J0510.0−6417
81.124	−69.686	280.365	−32.823	26	3.273	85.099	8.7	17.4	4.1	P4
81.395	−65.934	275.927	−33.308	6	3.516	21.094	2.8	6.4	1.7	N132D
e 82.289	−69.077	279.571	−32.520	34	2.542	86.424	14.3	26.3	3.4	N 49B
e 83.466	−69.436	279.920	−32.055	12	2.276	27.311	8.2	16.7	9.2	N49
84.258	−69.178	279.575	−31.810	57	4.200	239.427	9.0	25.1	6.5	FL8Y J0530.0−6900e
90.292	−70.566	280.993	−29.633	11	5.793	63.719	2.2	6.0	—	—
$\Lambda_{\text{cut}} = 0.5$										
77.435	−64.318	274.310	−35.209	16	3.999	63.988	3.2	10.0	2.3	FL8Y J0510.0−6417
81.231	−69.618	280.279	−32.798	17	4.008	68.133	4.8	15.2	2.1	P4
81.399	−65.933	275.923	−33.308	5	4.585	22.925	2.2	5.4	1.7	N132D
81.663	−69.251	279.816	−32.711	6	3.523	21.137	2.3	6.4	3.3	N 49B
82.763	−69.157	279.636	−32.341	5	4.040	20.200	2.0	5.3	9.5	N49
84.228	−69.174	279.573	−31.822	46	4.913	225.979	7.3	16.0	6.1	SNR B0528−692 ?
85.003	−69.303	279.686	−31.534	4	5.404	21.614	1.6	2.5	—	—
90.292	−70.566	280.993	−29.633	11	5.793	63.719	2.1	6.0	5.1	P2, N157B
									1.9	P1, PSR J0540−6919
									2.6	5BZQJ0601−7036

**Table 3** Coordinates and main properties of some low-significance MST clusters with  $M < 20$  detected in the LMC sky region at energies higher than 10 GeV (except for the latest entry, found at energies higher than 7 GeV). Celestial coordinates are J2000, angular distances  $\Delta\theta$  are computed between the centroids of MST clusters and those of indicated counterparts. See the main text for a discussion.

RA °	Dec °	$l$ °	$b$ °	$\Lambda_{\text{cut}}$	$N$	$g$	$M$	$R_m$ ′	$R_{\text{max}}$ ′	$\Delta\theta$ ′	Possible counterparts
69.500	−72.216	284.620	−35.709	0.6	4	3.379	13.515	1.6	6.8	—	—
73.854	−69.344	280.699	−35.373	0.6	4	3.726	14.905	2.0	3.8	5.9	3FGL J0456.2−6924
82.373	−72.715	283.801	−31.866	0.7	4	3.539	14.156	2.5	3.2	2.3	FL8Y J0529.3−7245
82.492	−68.491	278.871	−32.534	0.7	4	4.137	16.549	1.3	2.9	19.	3FGL J0526.6−6825e
82.952	−66.590	276.607	−32.605	0.5	4	4.077	16.307	1.9	4.7	3.6	FL8Y J0531.8−6639e
83.256	−69.342	279.823	−32.141	0.6	4	3.225	12.901	2.5	4.6	—	possible satellite
83.889	−66.119	276.006	−32.281	0.6	4	3.482	13.926	2.3	4.7	5.0	N 63A
										7.5	3FGL J0535.3−6559
77.921	−68.048	278.713	−34.278	0.6	4	2.915	11.658	2.9	5.3	1.2	FL8Y J0511.5−6803
83.888	−67.605	277.753	−32.129	0.7	4	1.849	7.397	4.5	6.2	2.8	P3, DEM L241
90.406	−72.613	283.343	−29.505	0.7	5	2.378	11.889	3.5	6.7	2.0	FL8Y J0601.3−7238
70.969	−66.884	278.210	−37.154	0.7	6	2.289	13.732	3.7	7.5	3.2	AllWISE CRATES

### 3.1 High significance clusters

The photon map in Figure 1 shows a sky region containing the LMC where the clusters selected by the MST analysis are reported together with other sources from the literature. It is apparent that the photon density is not homogeneous and that there is a higher concentration approximately around  $RA = 81^\circ$ ,  $Dec = -69^\circ$ , which includes the well known 30 Doradus complex (Foreman et al. 2015). In this region several contiguous clusters are found, marked by blue and red dots in the figure.

Centroid coordinates and other main parameters of the high significance ( $M \geq 20$ ) clusters selected with  $\Lambda_{\text{cut}} = 0.7$  are reported in the first part of Table 2, while in the second part are those found with  $\Lambda_{\text{cut}} = 0.5$ . In the former part there are 7 clusters (see also Figure 1), five of which have a positional correspondence with sources in the 3FGL catalogue (Acero et al. 2015) and with the sources found by Ackermann et al. (2016), which are indicated by P2 and P4. In the following we describe some of their properties and possible associations.

*MST(77.427, -64.315)*. This cluster is spatially close to the 3FGL J0509.7-6418, also reported as 1FHL J0509.9-6419, and a possible  $\gamma$ -ray source included in the preliminary 8-years source list<sup>3</sup> provided by the *Fermi*-LAT collaboration (also known as FL8Y), FL8Y J0510.0-6417, which does not have a well established counterpart: no known SNR is in close proximity, whereas it is associated with the bright X-ray source RBS 0625 (Schwope et al. 2000). This latter source has been classified as a quasar in the XMM-Newton Slew Survey (Warwick et al. 2012), and an interesting possibility is that it could be one of the background AGNs found in LMC.

*MST(81.124, -69.686)*. This rich cluster is closely associated with the other SNR N132D (source P4 in Ackermann et al. 2016) that is at an angular distance from the centroid less than  $2'$ .

*MST(82.289, -69.077)*. This cluster has a low  $g$  and the highest  $R_{\text{max}}$  and  $R_m$  values; on the basis of these values it is likely to be an extended structure (as indicated by the “e” in Table 2), and appears directly associated with the source FL8Y J0530.0-6900e,

also reported as extended in the preliminary *Fermi*-LAT list. Moreover, it is close to the other low  $g$  cluster MST(83.466, -69.436) and the sum of their  $R_{\text{max}}$ , equal to  $43'$ , is larger than the angular separation between their centroids ( $33'$ ), indicating that they can belong to a unique structure. Finally, note that the cluster centroid is moreover located between the two extended sources E1 and E3 reported by Ackermann et al. (2016).

*MST(84.258, -69.178)*. This is the richest cluster and is clearly associated with the SNR N157B (P2 source): the distance between the cluster centroid and the remnant is  $4'$ , compatible with instrumental PSF at these energies. However, the extension of this cluster is unusually large for a cluster having 57 photons, reaching a maximum radius  $R_{\text{max}}$  of  $25'$ , much larger than the X-ray size of the PWN, smaller than  $0.5$  (Wang et al. 2001). The analysis performed applying  $\Lambda_{\text{cut}} = 0.5$  (Table 2, lower section) gives again a rich cluster with 46 photons but a higher clustering factor and a shorter  $R_{\text{max}} = 16'$ , closer to the PSF size. Considering that this cluster is embedded in the major photon concentration it is likely that its extension can be originated by the aggregation of photons in the field, thus a more realistic structure of this cluster is that of a point-like structure embedded in an extended emission.

*MST(90.292, -70.566)*. This cluster can be the  $\gamma$ -ray counterpart of the blazar 5BZQ J0601-7036 (using the naming of the 5th Edition of the Roma-BZCAT of blazars, Massaro et al. 2014, 2015, also known as PKS 0601-70), corresponding to 3FGL J0601.2-7036. It is also reported in the FL8Y list.

There are two high significance clusters not associated to previously reported  $\gamma$ -ray sources, which show interesting peculiarities.

*MST(81.395, -65.934)*. This cluster has only 6 photons and a high  $g$  indicating a compact structure with a maximum radius of about  $6'$  as expected for a point-like source. It is at angular distance of  $3.4'$  from the SNR N 49B, while the nearby SNR N49 is at  $9.2'$ , both undetected by Ackermann et al. (2016). Considering its  $R_{\text{max}}$  the latter association appears quite unlikely. The analysis applying  $\Lambda_{\text{cut}} = 0.5$  (Table 2, lower section) substantially confirms this finding with a slightly reduced photon number but an increased  $g$ , thus giving the cluster an even higher magnitude value. The properties of this cluster and his association with the SNR N 49B will be discussed in detail in the following Section 4.

<sup>3</sup><https://fermi.gsfc.nasa.gov/ssc/data/access/lat/fl8y/>. Note that this catalog by no means official and will be soon superseded by the future 4FGL catalog.

*MST(83.466, -69.436)*. This is another structure with a low  $g$  and a large  $R_{\max}$ , inside the region with the highest photon concentration in the field, suggesting that it might be an extended feature, as previously observed for the cluster *MST(82.289, -69.077)*. To better understand its spatial structure, an analysis of the region with shorter values of  $\Lambda_{\text{cut}}$  is useful. With a separation length of 0.6 the cluster is divided in two not significant structures, one of which disappears when the separation length is reduced to 0.5. Thus the extended structure appears confirmed. There is no interesting counterpart, in particular no SNR in the Maggi et al. (2016) and Bozzetto et al. (2017) lists is close to this position. An interesting possibility that should be further investigated is that the extended cluster is originated by some weak point-like source embedded in a diffuse emission. For instance, the background quasar MQS J053242.46–692612.2 for which a spectroscopic redshift of 0.059 is reported (Kozłowski et al. 2013) and at about  $6'$  from the centroid, might be considered a possible candidate if it would exhibit a blazar nature. In fact, its classification appear somewhat uncertain because it is undetected in the radio band, but there is a corresponding source in the 1RXH, WGACAT (White et al. 2000), XMM and INTREFCAT (Ebisawa et al. 2003) catalogues, although it was early classified as Low Mass X-Ray Binary by Liu et al. (2001).

The results of cluster finding with  $\Lambda_{\text{cut}} = 0.5$  (Table 2, lower section) generally confirm the existence of all compact structures found with the larger separation length, with the addition of some new interesting clusters having a small number of photons but a  $g$  high enough to give a  $M$  value above the acceptance threshold. Their properties are described in the following.

*MST(81.663, -69.251)*. This cluster does not have any correspondence with any previously reported  $\gamma$ -ray sources. It is located near to the SNR B0528-692, whose X-ray diameter is  $3'3$  (Maggi et al. 2016), but the angular distance comparable to  $R_{\max}$  weakens the association; moreover, this SNR does not exhibit high brightness or other interesting properties, suggesting it as a powerful  $\gamma$ -ray emitter.

*MST(85.003, -69.303)*. This cluster of only 4 photons has an unusual high  $g$  and it is at a distance of only  $1'9$  to the young pulsar PSR J0540–6919, already reported as source P1 by Ackermann et al. (2016). A cluster of 7 photons and  $g = 4.33$  is found at  $3'$  from the pulsar using an intermediate length  $\Lambda_{\text{cut}} = 0.6$ , but no cluster is sorted out with longer separation values, because it is dispersed in the local background. The proposed very likely association with PSR J0540–6919 has

a rather soft spectrum, and could explain this marginal detection.

*MST(82.763, -69.157)*. This cluster corresponds to a cluster of 9 photons and a low  $g = 2.562$  with  $\Lambda_{\text{cut}} = 0.6$ , without any interesting counterpart. It can correspond to the extended sources E1 and E2 reported by Ackermann et al. (2016).

### 3.2 Low significance clusters

Several other clusters were not considered in the analysis carried out up to now, because their magnitude  $M$  was below the acceptance threshold and therefore the probability that they are random photon concentrations rather than features tracing genuine sources is generally higher than for the previous clusters. For a more complete description of the  $\gamma$ -ray emission structure of LMC, however, it is interesting to extend our analysis to these clusters. Moreover, we searched also if among other clusters sorted out by the MST there are some associations to sources already reported in the literature and mainly detected at lower energies. In first part of Table 3 are reported 7 clusters having only 4 photons,  $g \geq 3$  and, consequently,  $12 \leq M < 20$ . These clusters were found in the analyses with different  $\Lambda_{\text{cut}}$  and the reported parameters are those obtained with the highest  $M$ . The clusters and their centroids are also plotted in Figure 1. Note that four of these clusters are at a small angular distances from FL8Y (and also 3FGL) sources, indicating that these low  $M$  structures, but with high  $g$  values, must be taken into account for improving the completeness of search.

*MST(82.492, -68.491)*. This cluster is in the neighborhood of the highest density photon region and could be associated with an extended 3FGL source.

*MST(83.256, -69.342)*. It is located in the high density region and close to the boundary of the high significance cluster *MST(82.289, -69.077)* that can be associated with the source FL8Y J0530.0–6900e. A possibility to be taken into account is that it may be a *satellite* of the larger feature that is not connected to it because the occurrence of an edge just longer the separation length.

*MST(83.889, -66.119)*. It is the most interesting cluster in this list and a possible association with a near 3FGL source cannot be excluded, albeit at a distance larger than  $R_{\max}$ ; its centroid is, however, closer to the powerful SNR N 63A, for which Ackermann et al. (2016) reported only an upper limit to its  $\gamma$ -ray flux. A more complete analysis is given in the following Section 4.

For a more complete study on the possible sources in the LMC region we searched in our cluster lists if there are some interesting structures close to sources already reported in the literature and in other catalogues. Despite their low significance above 10 GeV, we found three more clusters, listed in the second part of the same Table 3, all close to FL8Y sources, two of which have  $M$  just below the threshold, while the third one has quite low  $g$  and  $M$ . Their individual properties are given in the following.

*MST(77.921, -68.048)*. This cluster is close to the source FL8Y J0511.5–6803 and its existence is confirmed by the analysis at energies higher than 5 GeV with  $\Lambda_{\text{cut}} = 0.7$  that gives a cluster of 8 photons with  $M = 18.262$  and an angular distance of only 1'.1 between their centroids.

*MST(83.888, -67.605)*. This cluster was detected above 10 GeV despite the very low clustering degree and corresponds to the candidate high-mass X-ray binary (HMXB) CXOUJ053600.0–673507 (Corbet et al. 2016), located in the supernova remnant DEM L241 (Seward et al. 2012). Moreover, it is close to the P3 source of Ackermann et al. (2016). The association of the  $\gamma$ -ray source with the X-ray binary is proved by the detection of a modulation of the  $\gamma$ -ray signal with the orbital period of 10.3 days, as measured from the radio, X-ray and radial velocity data (Corbet et al. 2016). The MST analysis at energies higher than 3 GeV with  $\Lambda_{\text{cut}} = 0.7$  gives at this location a cluster of 12 photons with  $M = 26.171$ , thus providing a satisfactory confirmation of our marginal high energy detection.

*MST(90.406, -72.613)*. This cluster has 5 photons and is located at only 2'.0 from the FL8Y J0601.3–7238; it has a very likely counterpart in the blazar candidate WIBRaLS J060141.32–723833.2 (D’Abrusco et al. 2014) at an angular distance from the centroid of 1'.8.

Finally, no cluster was found above 10 GeV close to the flat spectrum radio source LMC B0443–6657, or CRATES J044318–665155 (Healey et al. 2007), recently detected in the LAT data by Tang (2018). It should be emphasized that the spectral analysis by Tang (2018) gave above only upper limits above 10 GeV. A MST cluster search at energies higher than 7 GeV gave a low significance cluster whose parameters are given in the last section of Table 3. The CRATES source likely corresponds to an AGN (Secrest et al. 2015) with a relatively bright mid-infrared counterpart (AllWISE J044318.24–665204.4) whose (under-extended) colours are well located in the FSRQ region

of the *WISE* Gamma-ray blazar strip (D’Abrusco et al. 2013; Massaro and D’Abrusco 2016). On this basis, we conclude that the most likely counterpart of this source, if actually corresponding to that reported by Tang (2018), does not appear to be related to an LMC object but to a background FSRQ.

#### 4 The SNRs N 49B and N 63A: a more detailed analysis

Up to now, the only two SNRs in LMC firmly detected in the  $\gamma$ -ray band are N 132D and N 157B (Ackermann et al. 2016), while the same authors reported upper limits for other interesting sources of the same class (cf. their Table 6). Our MST analysis on the 9 year photon map above 10 GeV provided evidence for two clusters located very close to both the SNRs N 49B and N 63A. These clusters, however, have a rather low number of photons and it is then necessary to extend the analysis to confirm these findings.

A new MST analysis was performed in a  $6^\circ \times 6^\circ$  sub-region containing the two remnants, with different values of  $\Lambda_{\text{cut}}$  and extending the energy range down to 6 GeV. These searches confirmed the existence of clusters close to both N 49B and N 63A. Above 6 GeV a cluster at (81.3930, -65.9427), at the small angular separation of only 2'.7 from the former SNR, is found with 11 photons and  $M = 27.22$ , thus well above the significance threshold, while another and richer cluster is found at (83.9622, -66.1698), at a distance of 8'.0 from the latter SNR, with 9 photons and  $M = 30.21$ ,  $R_{\text{max}}$  being  $\sim 8'.1$  (the angular distance reduces to 5'.6 using the *unweighted* centroid). Using a lower energy threshold of 3 GeV an even richer cluster of 19 photons at (83.8927, -66.0977) with  $M = 51.58$  is found and its separation from the SNR decreases to 4'.6. The existence of reliable high energy  $\gamma$ -ray source candidates is then fully confirmed and the association with the two SNRs appears more robust. The photon map for  $E > 6$  GeV of a  $2^\circ \times 2^\circ$  region where the two SNRs are located is shown in Figure 2. Extracting from the sample of Maggi et al. (2016) the SNRs with a 0.3–8 keV X-ray luminosity brighter than  $7 \cdot 10^{33}$  erg/s, only 3 are within this field, the two under consideration and N 49. In the plot, the cluster photons are in blue (high significance clusters) and red (low significance clusters), while the crosses mark their centroid coordinates: it is clear that N 49 (orange circle) is outside the photon concentration while the association with N 49B is much more robust.

In this map it can be seen that both clusters have a pair of photons much closer between them than the

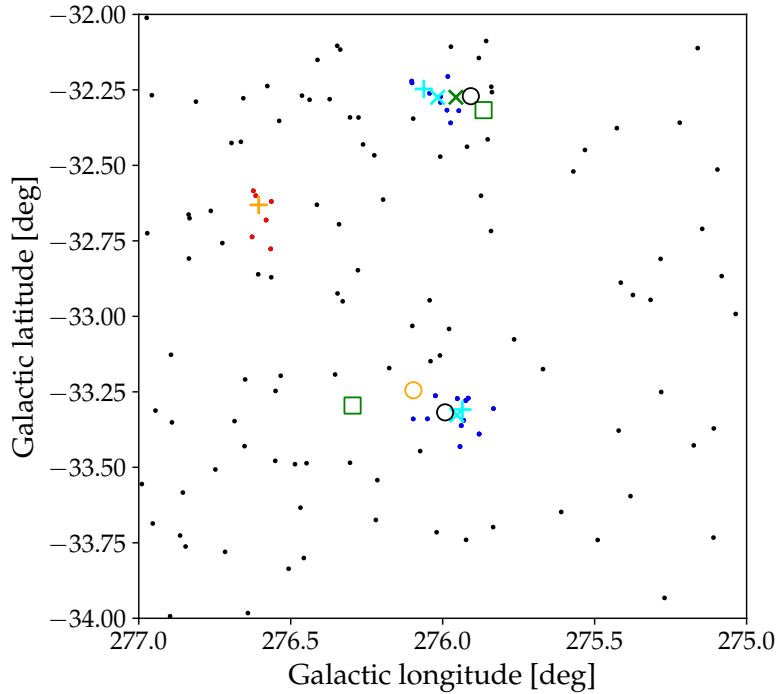


**Fig. 2** Photon map in Galactic coordinates of the sky region ( $2^\circ \times 2^\circ$ ) around SNR N 49B and N 63A at energies higher than 6 GeV. Photons are the black filled circles, while the blue ones correspond to the photons in the clusters found in the region with  $\Lambda_{\text{cut}} = 0.7$  and close to the SNRs (the upper one is around N 63A, while the lower one is around N 49B), and the red dots mark another low significance cluster. Cyan and orange pluses mark the weighted centroid positions, while cyan crosses are the unweighted centroid positions, and the green cross represents the centroid found for  $E > 3$  GeV. The positions of N 49B and N 63A are marked by black circles and N49 by an orange circle, respectively, while the green squares correspond to 3FGL sources.

other ones. This particular occurrence for cluster with a low photon number can slightly affect the estimates of the centroid coordinates, since they are weighted with the inverse of the squared edge length (see Campana et al. 2013, for a discussion). Therefore, it is useful to consider the *unweighted* centroids, also shown in Figure 2, which result closer to the location of the SNRs.

#### 4.1 Maximum Likelihood analysis

To validate the existence of a source and to estimate its photon flux, the standard binned Maximum Likelihood (ML) analysis was also performed at energies above 1 GeV in a sky region of interest (RoI) with an extension of  $10^\circ \times 10^\circ$  centered at the equatorial coordinates  $\alpha = 81^\circ.4$ ,  $\delta = -65^\circ.9$ .

In the case of LMC a major issue is the model for the local emission. Therefore, three possible models were considered beside the isotropic and Galactic diffuse backgrounds: *A*) 3FGL diffuse model for LMC (two 2D Gaussian spatial distributions for the full disk

and 30 Dor emission<sup>4</sup>) plus all the 3FGL point-like sources; *B*) the same model as *A*, but with the 3FGL sources inside the RoI replaced by the four sources reported by Ackermann et al. (2016) (P1–P4); *C*) like model *B*, but with the structured 4-component model derived by Ackermann et al. (2016) for the LMC diffuse emission<sup>5</sup>.

Spectral parameters for the background sources inside the RoI were fixed at their catalog values, with the exception of the flux normalisation. Moreover, two point-like sources with a power law spectrum were added to the model, with a location given by the MST centroid coordinates, leaving both the spectral index and the normalization as free parameters, in order to include the new MST-detected SNRs. Fit results are shown in Table 4.

Model *A* provided a significant detection for N 49B, with a test-statistics value of  $\sqrt{TS} = 6.6$  and a 1–

<sup>4</sup>Template available at [https://fermi.gsfc.nasa.gov/ssc/data/access/lat/4yr\\_catalog/LAT\\_extended\\_sources\\_v15.tgz](https://fermi.gsfc.nasa.gov/ssc/data/access/lat/4yr_catalog/LAT_extended_sources_v15.tgz).

<sup>5</sup>Templates available at [https://fermi.gsfc.nasa.gov/ssc/data/access/lat/3FHL/LAT\\_extended\\_sources\\_v18.tgz](https://fermi.gsfc.nasa.gov/ssc/data/access/lat/3FHL/LAT_extended_sources_v18.tgz).



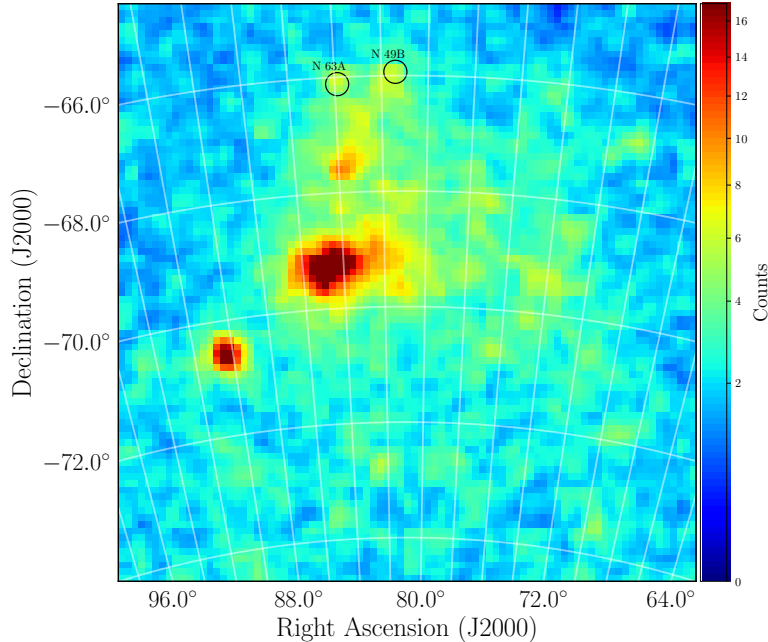


**Fig. 3** Count map of the wide-scale LMC  $\gamma$ -ray emission at energies higher than 1 GeV in equatorial coordinates, showing the locations of the two SNRs detected by MST (black circles): N 49B and N 63A are located just above and below the declination circle  $-66^\circ$ , respectively. Map with  $0^\circ.1$  wide pixels, smoothed with a Gaussian kernel one pixel wide based on 9-years *Fermi*-LAT data, and with a square-root color scale and Aitoff projection.

300 GeV flux of  $(2.7 \pm 0.7) \cdot 10^{-10}$  ph cm $^{-2}$  s $^{-1}$ . A source at the MST coordinates for N 63A is not detected, although the very close 3FGL J0535.3–6559 is detected with  $\sqrt{TS} = 8.0$ . We can conclude that the latter 3FGL source could be the counterpart of the MST cluster.

With Model *B* both sources are significantly detected, with  $\sqrt{TS}$  of 7.9 and 9.0 for N 49B and N 63A, respectively, with fluxes of  $(3.5 \pm 0.7) \cdot 10^{-10}$  and  $(3.4 \pm 0.6) \cdot 10^{-10}$  ph cm $^{-2}$  s $^{-1}$ .

With Model *C* however the detections are less significant, with  $\sqrt{TS}$  equal to 3.9 and 4.7, because the local excesses in correspondence to the two remnants can be partially blended in the highly structured LMC diffuse emission. Considering that the two SNRs are in a region of rather low diffuse local flux (see the count map in Figure 3) and quite distant from the prominent region of 30 Doradus, in particular at energies in the GeV band, the first two models are reasonably acceptable, and therefore ML results are not in conflict with our findings.

It is interesting to compare the Model *C* results to the 95% c.l. upper limits given by Ackermann et al. (2016), Table 6, for both SNRs. Assuming a power law index of 2, their upper limits are  $3.1 \cdot 10^{-7}$  and  $4.8 \cdot 10^{-7}$  MeV cm $^{-2}$  s $^{-1}$  for N 49B and N 63A in 1–10 GeV, respectively. Using the results in Table 4, we

obtain fluxes in the same band of  $(7 \pm 3) \cdot 10^{-7}$  and  $(9 \pm 3) \cdot 10^{-7}$  MeV cm $^{-2}$  s $^{-1}$ , respectively, i.e. about a factor of two higher than the upper limits given in Ackermann et al. (2016).

## 5 Summary and discussion

The Large Magellanic Cloud contains a large population of young SNRs, including Pulsar Wind Nebulae and shell-like structures (superbubbles) produced by blast waves sweeping out the ambient interstellar medium (Mac Low and McCray 1988), well observed in the radio band and X-ray bands (see, for instance, the recent papers by Maggi et al. 2016 and Bozzetto et al. 2017). H.E.S.S. observations in the TeV band (H.E.S.S. Collaboration et al. 2015) found the two powerful SNRs N 157B and N 132D, also detected by Ackermann et al. (2016) in the 6 year *Fermi*-LAT data. The latter authors were also able to detect two more point-like sources (P1 and P3): one identified as PSR J0540–6919, while the other one remained unassociated, and reported only upper limits for other powerful SNRs expected to be possible high energy emitters.

We analysed *Fermi*-LAT sky images, obtained in 9 years of observations at energies higher than 10 GeV,

**Table 4** Maximum likelihood results.  $\Gamma$  is the power law spectral index, and the flux is in the 1–300 GeV band. See main text for details.

Model	N 49B			N 63A		
	$\sqrt{TS}$	$\Gamma$	Flux [ph cm <sup>-2</sup> s <sup>-1</sup> ]	$\sqrt{TS}$	$\Gamma$	Flux [ph cm <sup>-2</sup> s <sup>-1</sup> ]
A	6.6	2.2 ± 0.2	(2.7 ± 0.7) · 10 <sup>-10</sup>	—	—	—
B	7.9	2.3 ± 0.2	(3.5 ± 0.7) · 10 <sup>-10</sup>	9.0	2.1 ± 0.2	(3.4 ± 0.6) · 10 <sup>-10</sup>
C	3.9	2.0 ± 0.3	(1.3 ± 0.6) · 10 <sup>-10</sup>	4.7	1.9 ± 0.2	(1.5 ± 0.5) · 10 <sup>-10</sup>

where the photon density is rather low, allowing a robust detection of photon clusters with typical sizes comparable or larger than the instrumental PSF. In the selection procedure rather severe threshold values were adopted to reduce the possibility of spurious detections originated by random fluctuations of background events. The application of MST provided 7 high significance clusters (Table 2), five of them clearly associated with known  $\gamma$ -ray sources, while the remaining two are without a correspondence in previous searches. One cluster has a quite large angular radius, indicative of an extended emission, while the other cluster, with only 6 photons but a rather high  $g$ , is found to have a positional correspondence with the SNR N 49B, up to now undetected in the  $\gamma$ -ray band. Moreover, a search performed using use of a shorter separation length  $\Lambda_{\text{cut}}$  provided three more clusters, one of which corresponding to the pulsar PSR J0540–6919 already reported by Ackermann et al. (2016), and another one in close proximity of the SNR B0528–692.

For the sake of completeness, our investigation was also extended to other structures classified as low significance clusters, containing only 4 or 5 photons and having magnitude values  $M < 20$  (Table 3). Seven other clusters were selected, four of them associated to previously known  $\gamma$ -ray sources. One of the three new clusters is located close to the SNR N 63A, and this association is strengthened by the finding of high significance clusters in analyses at lower energies.

The significance of the  $\gamma$ -ray emission from N 49B and N 63A was validated also by the ML analysis, with  $\sqrt{TS}$  values higher than the usual detection threshold of 5, although this result is dependent on the precise model assumed for the background sources in the region of interest.

Finally, we searched for clusters likely associated with other literature sources and found some structures with  $M$  values too low to be accepted as confirmed detections. A possible interpretation of these clusters is that they could be produced by very faint high energy sources, which above a few GeV would give only 2 or 3 photons in the considered timeframe, that grouped together with some background events are able to produce structures above the primary selection criteria.

It is interesting that clusters related to the source P3 by Ackermann et al. (2016) and to two FL8Y sources are found, besides the Tang (2018) source, whose likely counterpart appears to be a background blazar.

Considering the above results, the number of SNRs and PWNe in the LMC detected in the  $\gamma$ -ray band increases to four. As a final remark, no cluster was found corresponding to the position of SN 1987A confirming that the high energy emission in the GeV band from this object, if present, is much fainter than from older remnants.

We are grateful to the anonymous referee, whose careful reading of the manuscript and his/her useful comments greatly improved this paper. We acknowledge the use of archival *Fermi*-LAT data.

## References

- Acero, F., Ackermann, M., Ajello, M., Albert, A., Atwood, W.B., Axelsson, M., Baldini, L., Ballet, J., *et al.*: *Astrophys. J. Suppl. Ser.* **218**, 23 (2015)
- Ackermann, M., Ajello, M., Albert, A., Allafort, A., Atwood, W.B., Axelsson, M., Baldini, L., Ballet, J., *et al.*: *Astrophys. J. Suppl. Ser.* **203**, 4 (2012)
- Ackermann, M., Ajello, M., Allafort, A., Asano, K., Atwood, W.B., Baldini, L., Ballet, J., Barbiellini, G., *et al.*: *Astrophys. J.* **765**, 54 (2013)
- Ackermann, M., Albert, A., Atwood, W.B., Baldini, L., Ballet, J., Barbiellini, G., Bastieri, D., Bellazzini, R., Bissaldi, E., *et al.*: *Astron. Astrophys.* **586**, 71 (2016)
- Atwood, W., Albert, A., Baldini, L., Tinivella, M., Bregeon, J., Pesce-Rollins, M., Sgrò, C., Bruel, P., Charles, E., Drlica-Wagner, A., Franckowiak, A., Jogler, T., Rochester, L., Usher, T., Wood, M., Cohen-Tanugi, J., S. Zimmer for the Fermi-LAT Collaboration: *ArXiv e-prints* (2013). 1303.3514
- Bernieri, E., Campana, R., Massaro, E., Paggi, A., Tramacere, A.: *Astron. Astrophys.* **551**, 5 (2013)
- Bozzetto, L.M., Filipović, M.D., Vukotić, B., Pavlović, M.Z., Urošević, D., Kavanagh, P.J., Arbutina, B., Maggi, P., Sasaki, M., Haberl, F., Crawford, E.J., Roper, Q., Grieve, K., Points, S.D.: *Astrophys. J. Suppl. Ser.* **230**, 2 (2017)
- Campana, R., Massaro, E., Bernieri, E.: *Astrophys. Space Sci.* **361**, 367 (2016a)

- Campana, R., Massaro, E., Bernieri, E.: *Astrophys. Space Sci.* **361**, 185 (2016b)
- Campana, R., Massaro, E., Bernieri, E.: *Astrophys. Space Sci.* **361**, 183 (2016c)
- Campana, R., Massaro, E., Gasparrini, D., Cutini, S., Tramacere, A.: *Mon. Not. R. Astron. Soc.* **383**, 1166 (2008)
- Campana, R., Bernieri, E., Massaro, E., Tinebra, F., Tosti, G.: *Astrophys. Space Sci.* **347**, 169 (2013)
- Campana, R., Massaro, E., Bernieri, E., D'Amato, Q.: *Astrophys. Space Sci.* **360**, 19 (2015)
- Campana, R., Maselli, A., Bernieri, E., Massaro, E.: *Mon. Not. R. Astron. Soc.* **465**, 2784 (2017)
- Corbet, R.H.D., Chomiuk, L., Coe, M.J., Coley, J.B., Dubus, G., Edwards, P.G., Martin, P., McBride, V.A., Stevens, J., Strader, J., Townsend, L.J., Udalski, A.: *Astrophys. J.* **829**, 105 (2016)
- Cusumano, G., Maccarone, M.C., Mineo, T., Sacco, B., Massaro, E., Bandiera, R., Salvati, M.: *Astron. Astrophys.* **333**, 55 (1998)
- D'Abrusco, R., Massaro, F., Paggi, A., Masetti, N., Tosti, G., Giroletti, M., Smith, H.A.: *Astrophys. J. Suppl. Ser.* **206**, 12 (2013)
- D'Abrusco, R., Massaro, F., Paggi, A., Smith, H.A., Masetti, N., Landoni, M., Tosti, G.: *Astrophys. J. Suppl. Ser.* **215**, 14 (2014)
- Ebisawa, K., Bourban, G., Bodaghee, A., Mowlavi, N., Courvoisier, T.J.-L.: *Astron. Astrophys.* **411**, 59 (2003). [astro-ph/0309101](https://arxiv.org/abs/astro-ph/0309101). doi:10.1051/0004-6361:20031336
- Fermi LAT Collaboration, Ackermann, M., Albert, A., Baldini, L., Ballet, J., Barbiellini, G., Barbieri, C., Bastieri, D., Bellazzini, R., *et al.*: *Science* **350**, 801 (2015)
- Foreman, G., Chu, Y.-H., Gruendl, R., Hughes, A., Fields, B., Ricker, P.: *Astrophys. J.* **808**, 44 (2015)
- Ginzburg, V.L.: *Nature Physical Science* **239**, 8 (1972)
- Ginzburg, V.L., Ptuskin, V.S.: *Journal of Astrophysics and Astronomy* **5**, 99 (1984)
- Healey, S.E., Romani, R.W., Taylor, G.B., Sadler, E.M., Ricci, R., Murphy, T., Ulvestad, J.S., Winn, J.N.: *Astrophys. J. Suppl. Ser.* **171**, 61 (2007)
- H.E.S.S. Collaboration, Abramowski, A., Acero, F., Aharonian, F., Akhperjanian, A.G., Anton, G., Balenderan, S., Balzer, A., Barnacka, A., *et al.*: *Astron. Astrophys.* **545**, 2 (2012)
- H.E.S.S. Collaboration, Abramowski, A., Aharonian, F., Ait Benkhali, F., Akhperjanian, A.G., Angüner, E.O., Backes, M., Balenderan, S., Balzer, A., Barnacka, A., *et al.*: *Science* **347**, 406 (2015)
- Kozłowski, S., Onken, C.A., Kochanek, C.S., Udalski, A., Szymański, M.K., Kubiak, M., Pietrzyński, G., Soszyński, I., Wyrzykowski, L., Ulaczyk, K., Poleski, R., Pietrukowicz, P., Skowron, J., OGLE Collaboration, Meixner, M., Bonanos, A.Z.: *Astrophys. J.* **775**, 92 (2013)
- Liu, Q.Z., van Paradijs, J., van den Heuvel, E.P.J.: *Astron. Astrophys.* **368**, 1021 (2001). doi:10.1051/0004-6361:20010075
- Mac Low, M.-M., McCray, R.: *Astrophys. J.* **324**, 776 (1988)
- Maggi, P., Haberl, F., Kavanagh, P.J., Sasaki, M., Bozzetto, L.M., Filipović, M.D., Vasilopoulos, G., Pietsch, W., Points, S.D., Chu, Y.-H., Dickel, J., Ehle, M., Williams, R., Greiner, J.: *Astron. Astrophys.* **585**, 162 (2016)
- Marshall, F.E., Gotthelf, E.V., Zhang, W., Middleditch, J., Wang, Q.D.: *Astrophys. J. Lett.* **499**, 179 (1998)
- Massaro, E., Maselli, A., Leto, C., *et al.*: *Multifrequency Catalogue of Blazars*, 5th edn. Aracne Editrice, Rome (2014)
- Massaro, E., Maselli, A., Leto, C., Marchegiani, P., Perri, M., Giommi, P., Piranomonte, S.: *Astrophys. Space Sci.* **357**, 75 (2015)
- Massaro, F., D'Abrusco, R.: *Astrophys. J.* **827**, 67 (2016)
- Mattox, J.R., Bertsch, D.L., Chiang, J., Dingus, B.L., Digel, S.W., Esposito, J.A., Fierro, J.M., Hartman, R.C., Hunter, S.D., Kanbach, G., Kniffen, D.A., Lin, Y.C., Maccomb, D.J., Mayer-Hasselwander, H.A., Michelson, P.F., von Montigny, C., Mukherjee, R., Nolan, P.L., Ramana-murthy, P.V., Schneid, E., Sreekumar, P., Thompson, D.J., Willis, T.D.: *Astrophys. J.* **461**, 396 (1996)
- Schwöpe, A., Hasinger, G., Lehmann, I., Schwarz, R., Brunner, H., Neizvestny, S., Ugryumov, A., Balega, Y., Trümper, J., Voges, W.: *Astronomische Nachrichten* **321**, 1 (2000)
- Secrest, N.J., Dudik, R.P., Dorland, B.N., Zacharias, N., Makarov, V., Fey, A., Frouard, J., Finch, C.: *Astrophys. J. Suppl. Ser.* **221**, 12 (2015)
- Seward, F.D., Charles, P.A., Foster, D.L., Dickel, J.R., Romero, P.S., Edwards, Z.I., Perry, M., Williams, R.M.: *Astrophys. J.* **759**, 123 (2012)
- Sreekumar, P., Bertsch, D.L., Dingus, B.L., Fichtel, C.E., Hartman, R.C., Hunter, S.D., Kanbach, G., Kniffen, D.A., Lin, Y.C., Mattox, J.R., Mayer-Hasselwander, H.A., Michelson, P.F., von Montigny, C., Nolan, P.L., Pinkau, K., Schneid, E.J., Thompson, D.J.: *Astrophys. J. Lett.* **400**, 67 (1992)
- Tang, Q.-W.: *Astrophys. Space Sci.* **363**, 25 (2018)
- Wang, Q.D., Gotthelf, E.V., Chu, Y.-H., Dickel, J.R.: *Astrophys. J.* **559**, 275 (2001)
- Warwick, R.S., Saxton, R.D., Read, A.M.: *Astron. Astrophys.* **548**, 99 (2012)
- White, N.E., Giommi, P., Angelini, L.: *VizieR Online Data Catalog* **9031** (2000)